GliP, a Multimodular Nonribosomal Peptide Synthetase in *Aspergillus fumigatus*, Makes the Diketopiperazine Scaffold of Gliotoxin†

Carl J. Balibar and Christopher T. Walsh*

Department of Biological Chemistry and Molecular Pharmacology, Harvard Medical School, 240 Longwood Avenue, Boston, Massachusetts 02115

Received September 4, 2006; Revised Manuscript Received October 4, 2006

ABSTRACT: The fungal metabolite gliotoxin has a redox-active disulfide bridge spanning carbons 3 and 6 of a diketopiperazine (DKP) scaffold. The proposed DKP synthetase, GliP, from *Aspergillus fumigatus* Af293, is a three module (A_1-T_1-C_1-A_2-T_2-C_2-T_3) 236 kDa protein that can be overproduced in soluble form in *Escherichia coli*. Once primed on its three thiolation domains with phosphopantetheine prosthetic groups, GliP activates and tethers L-Phe on T_1 and L-Ser on T_2, before generating the L-Phe-L-Ser-*S*-T_2 dipeptidyl enzyme intermediate. Release of the dipeptide as the cyclic DKP happens slowly both in wild-type GliP and in enzyme forms where C_2 and T_3 have been mutationally inactivated. The lack of a thioesterase domain in GliP may account both for the slow release and for the directed fate of intramolecular cyclization to create the DKP scaffold for subsequent elaboration to gliotoxin.

The substituted 2,5-diketopiperazine (DKP)[1] gliotoxin (Figure 1A) is the prototypic secondary metabolite in a family of fungal toxins known as epipolythiodioxopiperazines (ETPs), which are characterized by an internal disulfide bridge (*1*). Gliotoxin, which is produced by various *Aspergillus*, *Gliocladium*, *Trichoderma*, *Candida*, and *Penicillium* species (*1*, *2*), has antiviral (*3*−*5*), antibacterial (*2*), and immunosuppressive (*6*−*8*) activity and causes apoptotic and necrotic cell death in vitro (*9*). These biological effects, as with all ETPs, are attributed to the bridged disulfide which mediates toxicity either by direct conjugation to proteins with susceptible thiol residues or by generating reactive oxygen species during redox cycling (*1*, *2*).

Rather little is known about the biosynthesis of gliotoxin and other ETPs. Feeding experiments have demonstrated that the core DKP is biosynthesized from phenylalanine (*10*) and serine (*11*); however, there has been some debate as to whether cyclo-(L-phenylalanyl-L-seryl) is an intermediate on the pathway to formation of gliotoxin. In support of such an intermediate, labeled Phe-Ser DKP has been efficiently incorporated into gliotoxin produced by *Trichoderma viride* (*12*, *13*), and protoplasts of *Gliocladium virens* can synthesize the dipeptide phenylalanylserine and the DKP cyclo-phenylalanylseryl (*14*). Contrarily, the mycelium of *Penicillium terlikowskii* poorly incorporates cyclo-phenylalanylseryl despite efficient uptake of the DKP (*15*). Furthermore, the protoplasts of *G. virens* which make the DKP do not biosynthesize gliotoxin (*14*), and an "intermediate trapping" experiment in *T. viride* showed that the cyclo-dipeptide may only be present in the organism in miniscule amounts under normal growth conditions (*13*). No other intermediates have been isolated on route to formation of gliotoxin.

DKPs are in themselves intriguing bioactive molecules. Several DKPs, cyclo(ΔAla-L-Val), cyclo(L-Pro-L-Tyr), and cyclo(L-Phe-L-Pro), isolated from cell-free supernatants of various Gram-negative bacteria, including *Enterobacter agglomerans*, *Citrobacter freundii*, and various *Pseudomonas* species, have been implicated in quorum sensing. All three of these DKPs are capable of activating a recombinant LuxR-based *N*-acylhomoserine lactone (AHL) biosensor in *Escherichia coli* as well as antagonizing the effect of the natural AHL activator, 3-oxo-C6-HSL. Additionally, cyclo(ΔAla-L-Val) and cyclo(L-Pro-L-Tyr) are capable of inhibiting the AHL-mediated swarming motility of *Serratia liquefaciens*, and cyclo(L-Pro-L-Tyr) is capable of activating another AHL biosensor in *Agrobacterium tumefaciens* (*16*). *Vibrio* spp. also produce cyclo(Phe-Pro), which affects the expression of the Tox-R-dependent genes ompU, ctxA, and ctxB, the latter two encoding subunits of cholera toxin which is involved in virulence of *Vibrio cholera* (*17*). DKPs can also act as antifungal compounds. Cyclo(L-Phe-L-Pro) and cyclo-(L-Phe-*trans*-4-OH-L-Pro) isolated from *Lactobacillus plantarum* have been shown to be active against *Fusarium sporotrichioides*, *Aspergillus fumigatus*, and *Kluyveromyces marxianus* (*18*). Finally, DKPs have been shown to be bactericidal as two marine bacterial strains associated with

† We gratefully acknowledge NIH Grant GM 20011 (to C.T.W.) and a Department of Defense National Defense Science and Engineering Graduate Fellowship (to C.J.B.).

* To whom correspondence should be addressed. E-mail: christopher_walsh@hms.harvard.edu. Phone: (617) 432-1715. Fax: (617) 738-0438.

[1] Abbreviations: DKP, diketopiperazine; ETP, epipolythiodioxopiperazine; AHL, *N*-acylhomoserine lactone; NRPS, nonribosomal peptide synthetase; A, adenylation; T, thiolation; C, condensation; PCR, polymerase chain reaction; SOE, splicing by overlap extension; IPTG, isopropyl β-D-1-thiogalactopyranoside; PP_i, pyrophosphate; PheA, adenylation domain construct of the PheATE module from gramicidin S synthetase; AMP, adenosine 5′-monophosphate; TE, thioesterase; HPLC, high-performance liquid chromatography; HOBt, hydroxybenzotriazole; HBTU, 2-(1*H*-benzotriazol-1-yl)-1,1,3,3-tetramethyluronium hexafluorophosphate; Fmoc, 9-fluorenylmethyl carbamate; LCMS, liquid chromatography mass spectrometry; SDS−PAGE, sodium dodecyl sulfate−polyacrylamide gel electrophoresis; DTT, dithiothreitol; BSA, bovine serum albumin; TCA, trichloroacetic acid; CoA, coenzyme A; DMF, *N*,*N*-dimethylformamide; DIEA, *N*,*N*-diisopropylethylamine; TFA, trifluoroacetic acid; TIS, triisopropylsilane.

10.1021/bi061845b CCC: $33.50
Published on Web 11/18/2006

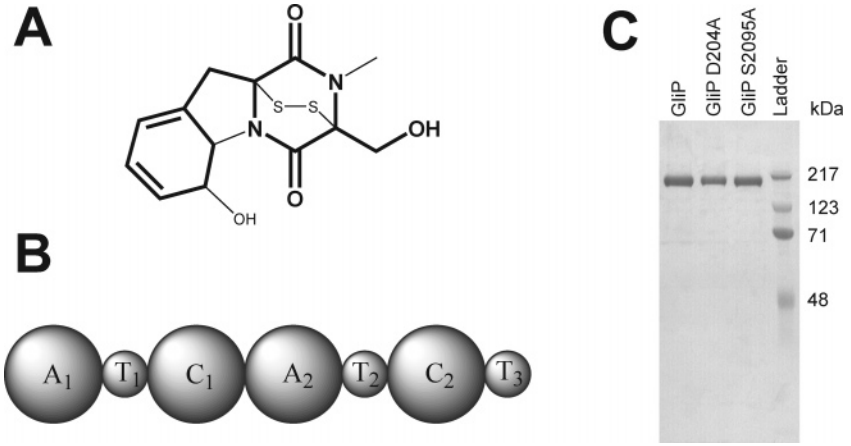

FIGURE 1: Gliotoxin structure and NRPS organization. (A) Structure of gliotoxin with the DKP core in bold. (B) Organization of the gliotoxin NRPS, GliP. (C) 10% SDS−PAGE gel of GliP wild-type protein and two representative GliP mutant proteins. The ladder is Bio-Rad prestained SDS−PAGE standards, high range.

cultures of *Pecten maximus* produce a series of five DD-DKPs that are active against *Vibrio anguillarum* (*19*).

Recently, the biosynthetic gene clusters of gliotoxin and a related ETP, sirodesmin, have been identified (*20*, *21*). Common to both clusters is a nonribosomal peptide synthetase (NRPS) with the architecture A-T-C-A-T-C-T, which is proposed to be responsible for forming the phenylalanylseryl DKP. It has recently been determined that disruption of this NRPS in *A. fumigatus* eliminates gliotoxin production (*22*).

NRPSs are multifunctional enzymes responsible for synthesizing a myriad of biologically active natural products (*23*−*26*). They are comprised of an assembly line of modules that utilize a thiotemplated (*27*) mechanism for the incorporation of monomers into an elongating peptidyl chain. Each module contains semiautonomous domains with either catalytic or carrier functions (*28*). Each adenylation (A) domain is responsible for substrate recognition and activation as an aminoacyl-*O*-AMP (*29*) with subsequent covalent loading onto a cognate thiolation (T) domain as an aminoacyl thioester (*30*, *31*). After initiation, a condensation (C) domain catalyzes peptide bond formation between two adjacent modules with nucleophilic attack of the downstream-loaded monomer on an upstream peptidyl thioester (*32*, *33*).

The gliotoxin NRPS, GliP, has an unanticipated domain architecture because it possesses an additional terminal C-T module (Figure 1B) that would not be expected to be necessary for formation of a dipeptide but could be involved for the subsequent transformation into a DKP. Furthermore, as noted in the examples above, it is rare for an NRPS to catalyze formation of a diketopiperazine that does not contain proline.

In this study we reconstitute the activity of the entire GliP NRPS in vitro and assay for the production of a phenylalanylseryl DKP intermediate. Due to the slow rate of DKP formation, we postulate that subsequent chemical transformations on route to gliotoxin, such as sulfur insertion, may occur while the linear dipeptide is still covalently bound to the NRPS, and release of the scaffold could occur from the terminal T domain of GliP at some later step.

EXPERIMENTAL PROCEDURES

Materials and General Methods. Standard recombinant DNA, molecular cloning, and microbiological procedures were performed as described (*34*). Competent Top10 and BL21(DE3) *E. coli* strains were from Invitrogen. Oligonucleotide primers were from Integrated DNA Technologies. Restriction enzymes and T4 DNA ligase were from New England Biolabs. Herculase DNA polymerase was from Stratagene. Plasmid pET24b was from Novagen. DNA sequencing to verify PCR fidelity was performed on double-stranded DNA by the Molecular Biology Core Facilities of the Dana Farber Cancer Institute (Boston, MA). Plasmid DNA preparation was performed using the Qiaprep kit from Qiagen. Gel extraction of DNA fragments as well as restriction endonuclease cleanup was done using the GFX kit from GE Healthcare. Ni-NTA Superflow resin was from Qiagen. FPLC purification of proteins was performed using a HiLoad 26/60 Superdex 200 prep grade column run on a P-920 pump equipped with a UPC-900 detector and a Frac-950 fraction collector (GE Healthcare) with a running buffer of 20 mM Tris, pH 8.0, 50 mM NaCl, 2 mM $MgCl_2$, and 1 mM DTT. SDS−PAGE gels were from Bio-Rad. Protein samples were concentrated using a 10K MWCO Amicon Ultra device from Millipore, and final protein concentrations were calculated using the protein's absorbance at 280 nm and the predicted molar extinction coefficient.

HOBt, HBTU, Fmoc-protected amino acids, and amino acid loaded resins were from NovaBiochem. Preparative HPLC was performed on a Beckman Coulter System Gold instrument with a Vydac Proteins and Peptides C18 column (10 μm, 22 × 250 mm). LCMS identification was carried out on a Shimadzu LCMS-QP8000α equipped with two LC-10ADVP liquid chromatography pump modules, a SPD-10AVVP UV−vis detector, a SIL-10ADVP autosampler module, and a Vydac C18 Mass Spec column (5 μM, 2.1 × 250 mm).

Radiolabeled L-[^{14}C]Ser (110 mCi/mmol) and L-[^{14}C]Phe (391 mCi/mmol) were from Sigma. Purified *Bacillus subtilis* phosphopantetheinyl transferase Sfp was obtained as previously described (*35*). Radio-HPLC was performed using a Beckman Coulter System Gold instrument equipped with a β-Ram module 3 radioisotope detector (IN/US Systems).

Phenylalanylseryl DKP was purchased from Sigma. Phe-Ser and Ser-Phe dipeptides were obtained from Bachem. All other chemicals and HPLC solvents were purchased from Sigma-Aldrich and were used without further purification.

Table 1: Primers Used To Generate GliP Mutants

GliP mutant	fragment	primer direction	primer sequence[a]
D204A	a	5′-forward	5′-*ACGCTCTGCCATA*TGCCATCAGTAGTAGCGCTCGAC-3′
		3′-reverse	5′-GAATGGAAAACAGCATGCCCGTAGAGGC*CGC*AAAGGATAC-3′
	b	5′-forward	5′-GTACTGCATATCCTGTCGGTATCCTTT*GCG*GCCTCTACG-3′
		3′-reverse	5′-GGAATCCGCGGTTCTTGACGGTGCGATCAC-3′
S555A	a	5′-forward	5′-GTAACGACGGCCAGCGCGTGGTGGAATTCC-3′
		3′-reverse	5′-GGGAGGTGAATCGAAGAGCAGCAAG*CGC*GTTTCCGCCC-3′
	b	5′-forward	5′-CAATTTCTTCGCCATGGGCGGAAAC*GCG*CTTGCTGCTC-3′
		3′-reverse	5′-CATTCGGTACATTGACATGTTGGATATCAG-3′
H757A	a	5′-forward	5′-GTAACGACGGCCAGCGCGTGGTGGAATTCC-3′
		3′-reverse	5′-CCCAGGGAGTAACCATCGATCAGGCT*CGC*GTGGGCCGTC-3′
	b	5′-forward	5′-GAAGTGACTGTCGTCTGGACGGCCCAC*GCG*AGCCTGATC-3′
		3′-reverse	5′-CATTCGGTACATTGACATGTTGGATATCAG-3′
D1254A	a	5′-forward	5′-GGCCGACAAAAGCACCGCTTGCCGTCGACC-3′
		3′-reverse	5′-CGCAGAGAAAATCTCGTTGGCACAGTA*CGC*GAACGCAGG-3′
	b	5′-forward	5′-GTATAGCTCAGTTCATGTCGCCTGCGTTC*GCG*TACTGTGCC-3′
		3′-reverse	5′-CTCTTGGTACATCTTCTGCTCGACCGCCGC-3′
S1582A	a	5′-forward	5′-CGGCAGGTCAAAATCCGTGGCTTCCGCGTC-3′
		3′-reverse	5′-GAGCCGCCAACATCATCTGGAGAAC*CGC*ATGGCCGCCC-3′
	b	5′-forward	5′-GATGACTTCCGTGCTCTGGGCGGCCAT*GCG*GTTCTCCAG-3′
		3′-reverse	5′-*CGTGTGGAACTCGAG*AAGAACCTGACGGTAAAGACG-3′
H1754A	a	5′-forward	5′-CGGCAGGTCAAAATCCGTGGCTTCCGCGTC-3′
		3′-reverse	5′-GCACGCTGTTGAGATCGGCGACGGCCG*CGC*TGGTAACC-3′
	b	5′-forward	5′-GTCGCACCCTCCTTGTGGTTACCAGC*GCG*GCCGTCGCCG-3′
		3′-reverse	5′-*CGTGTGGAACTCGAG*AAGAACCTGACGGTAAAGACG-3′
T1778P	a	5′-forward	5′-CGGCAGGTCAAAATCCGTGGCTTCCGCGTC-3′
		3′-reverse	5′-GGGATAGTGCCATCGGTCCGGTGTTGG*CGG*CGTCCTTCC-3′
	b	5′-forward	5′-GTCTCCGGCGTGTACGCGGGAAGGACG*CCG*CCAACACCG-3′
		3′-reverse	5′-*CGTGTGGAACTCGAG*AAGAACCTGACGGTAAAGACG-3′
S2095A	a	5′-forward	5′-CGGCAGGTCAAAATCCGTGGCTTCCGCGTC-3′
		3′-reverse	5′-GACGGCTCAACCGCCAGGCCTGGAT*CGC*GTCGCCGCCG-3′
	b	5′-forward	5′-GTCTCCTTCTTCGAGGCCGGCGGCGAC*GCG*ATCCAGGCC-3′
		3′-reverse	5′-*CGTGTGGAACTCGAG*AAGAACCTGACGGTAAAGACG-3′

[a] Italic, modified sequences; underlined, restriction site.

Cloning of GliP and Mutants, Overproduction, and Purification of GliP Proteins. The wild-type GliP construct was obtained from PCR amplification of *A. fumigatus* Af293 cDNA, which was a gift from Robert A. Cramer, Jr., Durham, NC (*22*). Due to PCR difficulties and the need to remove an internal *Xho*I site from the GliP sequence, the construct was amplified from this template in three pieces and then ligated together. The following oligonucleotide primers were used (italic, modified sequences; underlined, restriction site): GliP(a), 5′-*ACGCTCTGCCATA*TGCCATCAGTAGTAGCGCTCGAC-3′ and 5′-CGCTGGGGAGCCCCCTC*C*AGATACTTCGACCAGAAC-3′; GliP(b), 5′-GCTCACGGGGCCGACAAAAGCACCGCTTGC-3′ and 5′-CGGGATGTCCAGACGCTGGGGAGCCCCCTC*C*AGATACTTC-3′; GliP(c), 5′-GGAACGGAAGTTCTGGTCGAAGTATCT*G*GAGGGGGC-3′ and 5′-*CGTGTGGAACTCGAG*AAGAACCTGACGGTAAAGACG-3′. To incorporate the C5424G mutation, the splicing by overlap extension method (*36*) was used with the GliP(b) and GliP(c) fragments. After PCR purification, the two fragments were mixed together and further amplified using the forward first primer from GliP(b) and the reverse second primer from GliP(c), yielding a GliP(bc) product. GliP(a) was digested with *Nde*I/*Hin*dIII and ligated into a similarly digested pET24b vector. GliP(bc) was digested with *Hin*dIII/*Xho*I and ligated into a similarly digested pET24b vector. After sequencing, a correct GliP(bc) clone was digested again with *Hin*dIII/*Xho*I and ligated into a similarly digested pGliP(a) pET24b vector to give a full pGliP plasmid yielding a C-terminal His_6-tagged construct.

All GliP mutants were derived using pGliP as template and SOE with the primers listed in Table 1. After PCR purification the a and b fragments for each mutant were mixed together and further amplified using the 5′-forward first primer from the a fragment and the 3′-reverse second primer from the b fragment. The final PCR product GliP(D204A) was digested with *Nde*I/*Not*I, GliP(S555A) and GliP(H757A) were digested with *Not*I/*Hin*dIII, GliP(D1245A) was digested with *Hin*dIII/*Sac*I, and GliP(S1582A), GliP(H1754A), GliP(T1778P), and GliP(S2095A) were digested with *Sac*I/*Xho*I and ligated into a similarly digested pGliP plasmid.

The described expression plasmids were transformed into *E. coli* BL21(DE3) competent cells. All constructs were grown at 15 °C in Luria−Bertani media supplemented with 5 mM $MgCl_2$ and 40 μg/mL kanamycin to an OD_{600} of 0.8 when the culture was induced with 100 μM IPTG and then grown for an additional 24 h. The cells were harvested by centrifugation at 4000*g* for 16 min and stored as pellets at −80 °C until further use. Cell pellets from 6 L of culture were thawed and resuspended in 30 mL of buffer (25 mM Tris, pH 8.0, 500 mM NaCl) and then lysed with two passes on an Emulsiflex-C5 cell disruptor (Avestin). The lysate was cleared by ultracentrifugation at 95000*g* for 35 min and then transferred to 1 mL of Ni-NTA resin for incubation at 4 °C for 1.5 h. The resin was then transferred to a column, and the protein was eluted with an imidazole gradient using steps of 25 mL of 0 and 5 mM imidazole, 25 mL of 25 mM imidazole, 10 mL of 200 mM imidazole, and 5 mL of 500 mM imidazole mixed into lysis buffer. After an SDS−PAGE

gel was run to verify which fractions contained the protein, the 25, 200, and 500 mM imidazole fractions were concentrated to 1.5 mL and subjected to gel filtration purification. After the fractions containing the protein of interest were confirmed using SDS−PAGE, the resulting fractions were concentrated, supplemented with 10% glycerol, flash frozen in liquid nitrogen, and stored at −80 °C.

ATP−PP_i Exchange Assay for GliP A Domain Substrate Specificity. Reactions (100 μL) contained 75 mM Tris, pH 7.5, 10 mM $MgCl_2$, 5 mM DTT, 5 mM ATP, 1 mM sodium [^{32}P]pyrophosphate (0.18 μCi), 100 μg/mL BSA with 0.1 μM enzyme, and substrate amino acid concentrations ranging from 0.05 to 17 mM. Reactions were incubated at room temperature for 12 min and were quenched by addition of 500 μL of 1.6% (w/v) activated charcoal, 200 mM tetrasodium pyrophosphate, and 3.5% perchloric acid in water. The charcoal was pelleted by centrifugation and washed twice with 500 μL of 200 mM tetrasodium pyrophosphate and 3.5% perchloric acid in water. The radioactivity bound to the charcoal was then measured by liquid scintillation counting. Note that enzyme concentrations and reaction times were chosen such that ATP−PP_i exchange remained under 10% of equilibrium levels.

Analysis of Phosphopantetheinylation of Apo T Domain Constructs. Reactions (20 μL) to determine whether the T domains were functional for phosphopantetheinylation contained 75 mM Tris, pH 7.5, 5 mM $MgCl_2$, 100 μM [^{14}C]-acetyl-CoASH, and 10 μM GliP and were initiated with 3 μM Sfp. At various time points ranging from 1 min to 5 h, reactions were quenched into 80 μL of 10% TCA. Samples were centrifuged and washed with 2 × 200 μL of 10% TCA, and the protein pellet containing covalently bound radiolabeled CoA was resolubilized in 200 μL of formic acid and quantified by liquid scintillation counting. Acetyl-CoASH was used instead of the natural CoASH substrate because of the ability to incorporate a ^{14}C radiolabel on the acetyl group. This radiolabel enables the monitoring of any pantetheine prosthetic group that is covalently appended to the NRPS by Sfp.

Synthesis of Peptide Standards: L-*Ser*-L-*Phe*-L-*Ser*, L-*Phe*-L-*Ser*-L-*Phe*-L-*Ser*, L-*Phe*-L-*Phe*-L-*Ser*, L-*Phe*-L-*Phe*-L-*Phe*-L-*Ser, and* L-*Phe*-D-*Ser*. H-Ser(OtBu)-2-ClTrt resin or D-Ser-(OtBu)-Wang resin was swelled in DMF and then reacted with 3 equiv of F-moc protected amino acid, 3 equiv of HBTU, 1 equiv of HOBt, and 12 equiv of DIEA dissolved in enough DMF to bring the 3 equiv of amino acid to be coupled to 0.2 M while shaking at room temperature for 2.5 h. Afterward, the resin was washed with 3 × 3 mL of DMF and 3 × 3 mL of CH_2Cl_2 followed by F-moc deprotection with 2 × 3 mL of 20% piperidine for 20 min.

After the resin was washed with another 3 × 3 mL of DMF and 3 × 3 mL of CH_2Cl_2, the procedure was repeated again if there was another amino acid to be coupled. Otherwise, the product was cleaved from the resin overnight using 2 mL of 90/5/5 TFA/H_2O/TIS. The TFA was blown off under a stream of nitrogen, and the product was redissolved in H_2O and purified by preparative HPLC using a gradient of 0−25% acetonitrile over 25 min starting in 0.1% TFA in H_2O. Product peaks were identified by LCMS and lyophilized to dryness.

Analysis of Intermediates Tethered to GliP. Each GliP enzyme (10 μM) included in the 120 μL reaction was primed by incubation with 75 mM Tris, pH 7.5, 5 mM $MgCl_2$, 300 μM CoASH, and 3 μM Sfp at room temperature for 1 h. Amino acid loading and condensation were then assayed by initiation with 37.5 mM Tris, pH 7.5, 5 mM ATP, and 400 μM of each amino acid included (both ^{14}C radiolabeled and unlabeled). After 1.5 h, reactions were quenched in 480 μL of 10% TCA, pelleted by centrifugation, and washed with 3 × 100 μL of 10% TCA. Cleavage of the T domain bound products was performed by resuspending in 100 μL of 0.1 M LiOH and heating at 60 °C for 15 min. The reaction was then quenched by acidifying with 20 μL of 50% TCA and centrifuged to pellet the protein. The supernatant containing the released products was analyzed by HPLC on a Vydac 250 × 4.6 mm C18 small pore column, using a 0−18% acetonitrile gradient over 18 min, then holding for an additional 10 min, starting in 0.1% TFA in H_2O, and monitoring ^{14}C radioactive counts and absorbance at 260 nm.

Analysis of DKP Released from GliP. Each GliP enzyme (10 μM) included in the 20 μL reaction was primed by incubation with 75 mM Tris, pH 7.5, 5 mM $MgCl_2$, 300 μM CoASH, and 3 μM Sfp at room temperature for 1 h. The reaction was then initiated with 37.5 mM Tris, pH 7.5, 5 mM ATP, 400 μM unlabeled L-Phe and 400 μM ^{14}C radiolabeled L-Ser. At desired time points, reactions were quenched in 80 μL of 10% TCA and pelleted by centrifugation, and the supernatant containing the released DKP product was analyzed by HPLC on a Vydac 250 × 4.6 mm C18 small pore column, using a 0−18% acetonitrile gradient over 18 min, then holding for an additional 10 min, starting in 0.1% TFA in H_2O, and monitoring ^{14}C radioactive counts.

RESULTS

Cloning and Expression of GliP Constructs. The gliotoxin NRPS, GliP, was amplified from cDNA derived from mycelial tissue of *A. fumigatus* Af293. In order to facilitate cloning into a C-terminal His_6-tagged vector, an internal *Xho*I site had to be removed from the GliP sequence. Therefore, a silent C5424G mutation was introduced during the PCR process. Sequencing of pGliP revealed that although the two introns predicted by bioinformatics (*20*) were present, the first was 30 nucleotides too long. The corrected GliP sequence has been deposited in GenBank (accession number DQ457015). All GliP point mutants, D204A (A_1), S555A (T_1), H757A (C_1), D1245A (A_2), S1582A (T_2), H1754A (C_2), and S2095A (T_3), were derived from this pGliP construct and generated using the splicing by overlap extension (SOE) method (*36*). Expression in *E. coli* at 15 °C with 0.1 mM IPTG induction yielded 3−4 mg/L protein for all constructs. All of the 236 kDa proteins were purified to homogeneity using nickel-affinity chromatography and gel filtration in tandem (Figure 1C).

Amino Acid Activation and Loading. Due to the cyclic nature of the DKP scaffold in gliotoxin, the specificities of the two A domains of GliP were unknown as cyclization could arise from either a L-Phe-L-Ser or a L-Ser-L-Phe dipeptidyl-*S*-T domain precursor. Absent prediction from colinearity with the released peptidyl product, the specificities of A domains in NRPS modules have traditionally been deduced using an NRPS code in which the identity of eight amino acids in the A domain between a conserved aspartate and lysine confers substrate specificity (*37*). However, this

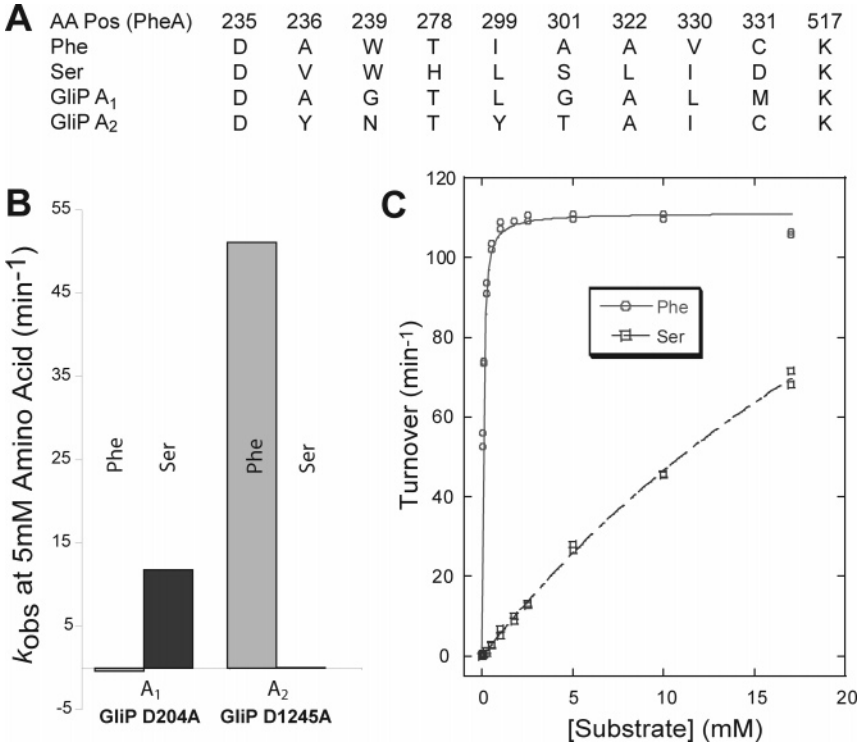

FIGURE 2: Analysis of GliP A domains. (A) Alignment of the two A domains of GliP with amino acid residues predicted to confer specificity for L-Phe and L-Ser according to the NRPS A domain code based on residue positions within PheA. (B) Activation of L-Phe and L-Ser by the GliP A domain mutants D204A (A_1) and D1245A (A_2). (C) Michaelis−Menten kinetic parameters for activation of L-Phe and L-Ser by wild-type GliP. Light gray represents L-Phe and dark gray represents L-Ser.

code appears to only be applicable to bacteria and has not been generalizable to fungal A domains (*38*), as noted in Figure 2A.

In order to address the functionality and specificity of the two GliP A domains, an ATP−PP_i exchange assay was performed to determine whether the A domains were capable of converting amino acid substrate into an aminoacyl-*O*-AMP. To distinguish which A domain activates L-Phe and which activates L-Ser, point mutants were constructed in A_1 (D204A) or A_2 (D1245A) to selectively knockout a given A domain and test only the activity of the remaining one. The conserved aspartate side chain in question is known from crystal structures (*29*) to charge pair with the positively charged NH_3^+ of the amino acid substrate. As noted in Figure 2B, the D204A mutant was capable of activating L-Ser, but not L-Phe, and conversely, the D1245A mutant was capable of activating L-Phe, but not L-Ser. These results conclusively establish that A_1 activates L-Phe and A_2 activates L-Ser and make the strong prediction that a L-Phe-L-Ser-*S*-GliP is the precursor to the cyclo-L-Phe-L-Ser DKP of gliotoxin.

Once the substrate specificities were established for the two A domains and it was determined that neither would activate the other's substrate, a full set of Michaelis−Menten parameters for the amino acid-dependent PP_i−ATP exchange by wild-type GliP was performed. As seen in Figure 2C the k_{cat} for A_1 toward L-Phe was 111.2 ± 0.6 min^{-1} and the K_m was 51 ± 2 μM. The kinetics of A_2 toward its substrate L-Ser were far worse with a k_{cat}/K_m of 5.44 ± 0.08 mM^{-1} min^{-1}, which is approximately 4×10^6-fold lower than the catalytic specificity of A_1 toward L-Phe. Although the calculated K_m was higher than the maximum 17 mM concentration of L-Ser tested, the estimated k_{cat} was 240 ± 20 min^{-1} and the estimated K_m was 40 ± 4 mM. Given these results of low affinity for L-Ser, several other amino acids were tested for activation by A_2 to determine whether L-Ser was the actual precursor amino acid used in formation of the gliotoxin DKP scaffold. However, no activation was seen with the amino acids D-Ser, L-Ala, Gly, or L-Cys (data not shown). The PP_i−ATP exchange measures both the back and forward reaction, involving PP_i release and readdition to the aminoacyl-AMP enzyme complex. It is possible that PP_i release is limiting in this assay.

Detection of Covalent Aminoacyl- and Dipeptidyl-S-Enzyme Intermediates. GliP has three putative 10 kDa thiolation domains embedded in its 2136 residue sequence, with Ser_{555}, Ser_{1582}, and Ser_{2095} as the proposed sites for posttranslational priming with phosphopantetheine to convert inactive apo T domains into active holo T domains. A dedicated phophopantetheinyl transferase for such posttranslational priming is not detectable in the GliP cluster (*20*) so the broad specificity *B. subtilis* Sfp enzyme (*35*) was utilized to prime GliP for subsequent studies. Using a ratio of 1/3 Sfp/GliP, close to maximal phosphopantetheinylation was achieved within 5 min (data not shown).

With three T domains and only two A domains, it was unknown whether GliP conformed to the rule of colinearity followed by most NRPSs (*39*). Following the formation of Phe-AMP and Ser-AMP in the active sites of the two A domains, the activated amino acid moieties should be transferable to the HS-pantetheinyl arm of the immediate downstream T domain. To address this question, an alanine point mutant of the conserved phosphopantetheinylated serine was made for each of the three T domains. After initial experiments using either L-[^{14}C]Phe or L-[^{14}C]Ser positively demonstrated covalent loading of the radioactive aminoacyl group on holo T forms of wild-type GliP, mixtures of these

amino acids, both radiolabeled and unlabeled, were used to interrogate T domain function.

As can be seen in Figure 3A,B, when either L-[^{14}C]Phe and unlabeled L-Ser or L-[^{14}C]Ser and unlabeled L-Phe were mixed with holo GliP, the thioester linkages cleaved by base treatment, and the products detected by HPLC analysis, the L-Phe-L-Ser dipeptide was recovered. If the T_1 domain is mutated, L-Phe cannot be loaded, and no dipeptide is formed; however, L-Ser is still able to be loaded. Conversely, when T_2 is mutated, L-Ser cannot be loaded, the dipeptide again is not formed, but L-Phe can still be loaded. Mutation of T_3 does not affect loading of L-[^{14}C]Phe, L-[^{14}C]Ser, or dipeptide formation. These results conclusively demonstrate that A_1 loads L-Phe onto T_1 and A_2 loads L-Ser onto T_2, with subsequent dipeptide condensation occurring, presumably by action of C_1. To verify this, an alanine point mutation was created in the conserved catalytic His motif of C_1 at H_{757} (*40*). As predicted, in the absence of functional C_1, L-Phe and L-Ser can be loaded, but no dipeptide is formed (Figure 3C).

Diketopiperazine Release and Roles of C_2 and T_3. Two additional features of GliP (A_1-T_1-C_1-A_2-T_2-C_2-T_3) are of note. First, it has a third putative module (C_2-T_3) that is noncanonical in that it lacks an A domain of typical NRPS elongation modules (*39*). Second, although the cyclic DKP is the anticipated product to be released by GliP, there is no discernible thioesterase (TE) domain (*39*) at the carboxy terminus of GliP. The great majority of NRPS assembly lines end in a TE domain that catalyzes the disconnection of the full-length acyl chain from its thioester linkage to the pantetheinyl arm of the most downstream T domain (*41*).

The question arises whether the dipeptidyl L-Phe-L-Ser chain is moved from T_2 to T_3 by C_2 action not as a peptide synthetase but as an acyl (dipeptidyl) transferase and whether that leads to release by intramolecular cyclization as the DKP. To study this question, the S2095A T_3 and the H1754A C_2 GliP mutants were analyzed. As discussed above, after base hydrolysis of tethered products, the T_3 mutant releases L-Phe-L-Ser dipeptide present on T_2, L-Phe that has been reloaded onto T_1, as well as two additional products (Figure 4A). Both of these new peaks are visible when either L-Ser or L-Phe is radiolabeled, indicating that the products contain at least one of each of these amino acids.

The first of these peaks was positively identified as the L-Phe-L-Ser DKP by both coelution with authentic standard (Figure 4B) and mass spectral analysis: 235.10 $[M + H]^+$ calculated, 234.8 observed. Formation of radiolabeled DKP suggests that failure to transfer the chain to T_3 may result in stalling and a conformation of GliP that results in intramolecular capture of the activated L-Ser carbonyl by the amino group of the L-Phe-L-Ser-*S*-T_2 during base hydrolysis. The inactive C_2 mutant gives the same pattern as the inactive T_3 mutant (Figure 4A), consistent with the view that C_2 and T_3 are involved in the same process: they may normally move the dipeptidyl moiety from T_2 to T_3, and when that does not occur, DKP formation ensues under these experimental conditions. Unfortunately, the second peak was not yet able to be identified. Several possible compounds were synthesized to check for identity by coelution, including L-Ser-L-Phe, L-Ser-L-Phe-L-Ser, L-Phe-L-Ser-L-Phe-L-Ser, L-Phe-L-Phe-L-Ser, L-Phe-L-Phe-L-Phe-L-Ser, and L-Phe-D-Ser, none of which were positive matches (Figure 4C). Collection

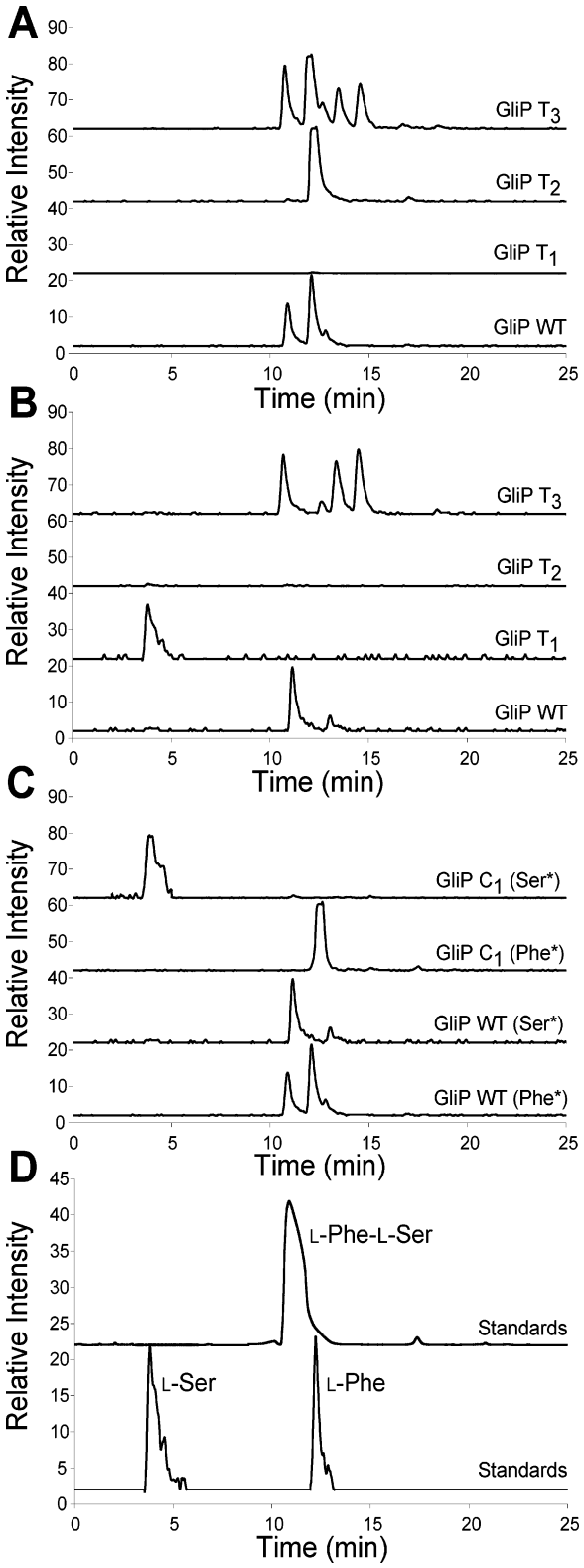

FIGURE 3: Analysis of GliP T domains. (A) Radio-HPLC traces depicting intermediates tethered to wild type and designated GliP T domain mutants when L-[^{14}C]Phe and unlabeled L-Ser are loaded onto GliP. (B) Radio-HPLC traces depicting intermediates tethered to wild type and designated GliP T domain mutants when L-[^{14}C]-Ser and unlabeled L-Phe are loaded onto GliP. (C) Radio-HPLC traces depicting intermediates tethered to wild type and a C_1 GliP mutant when L-[^{14}C]Phe and unlabeled L-Ser (Phe*) or L-[^{14}C]Ser and unlabeled L-Phe (Ser*) are loaded onto GliP. (D) HPLC traces showing designated standards with which GliP intermediates coelute. L-Phe and L-Ser were monitored by ^{14}C radioactive counts, and L-Phe-L-Ser dipeptide was monitored at 260 nm.

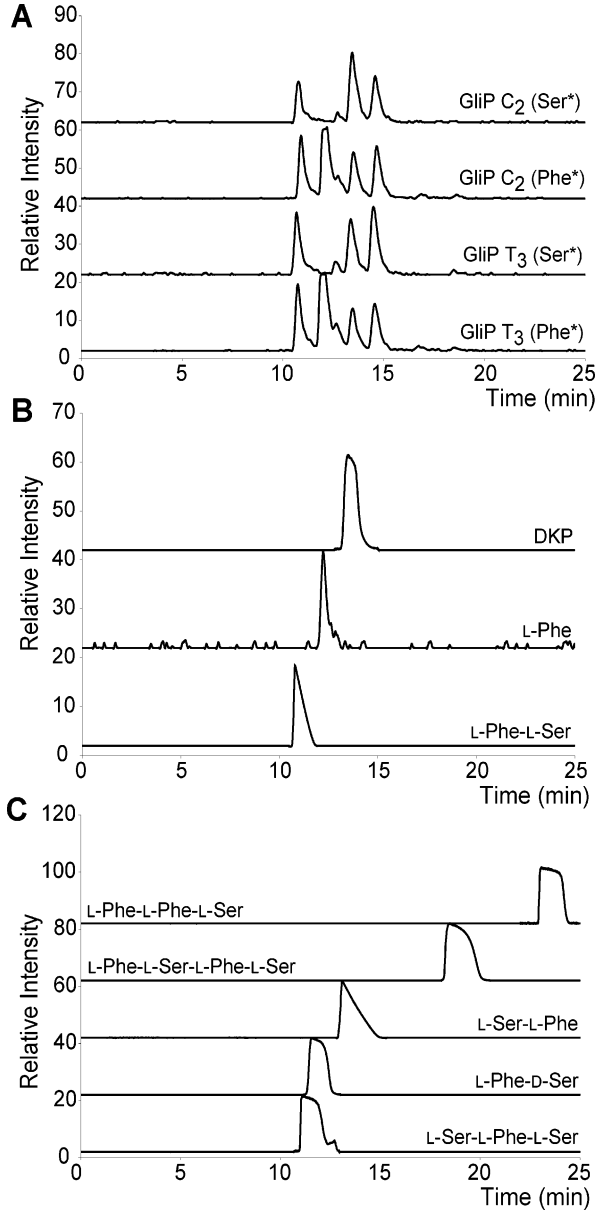

FIGURE 4: Analysis of GliP C_2 and T_3 mutants. (A) Radio-HPLC traces depicting intermediates tethered to a C_2 and T_3 GliP mutant when L-[^{14}C]Phe and unlabeled L-Ser (Phe*) or L-[^{14}C]Ser and unlabeled L-Phe (Ser*) are loaded onto GliP. (B) HPLC traces showing designated standards with which GliP mutant intermediates coelute. L-Phe was monitored by ^{14}C radioactive counts, and L-Phe-L-Ser dipeptide and phenylalanylseryl DKP were monitored at 260 nm. (C) HPLC traces showing compounds which could have identified the fourth unknown peak but did not coelute. All standards were monitored at 260 nm. Not shown is the L-Phe-L-Phe-L-Phe-L-Ser compound which eluted at 29 min in the given conditions.

of the peak for identification by mass spectrometry was also unsuccessful. At most, it is known that the unknown product contains Phe and Ser, and probably does not contain more than one Phe, since all compounds with more than one Phe are retained on the C18 small pore HPLC column much longer than the unknown peak.

Finally, the rate of DKP formation was tested for wild-type GliP as well as the C_2 and T_3 mutants. If the DKP is an actual intermediate on the pathway to gliotoxin formation, it would be expected that GliP would form and release the molecule at a reasonable enzymatic rate. As can be seen in Figure 5, DKP formation is not fast, occurring at a rate of

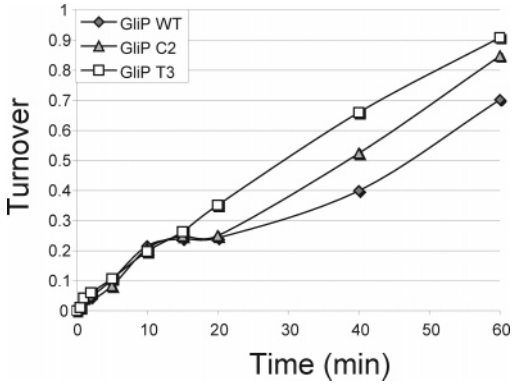

FIGURE 5: DKP formation. Time course showing soluble DKP released from wild-type GliP and C_2 and T_3 mutants. Diamonds represent wild-type GliP, triangles represent the GliP C_2 mutant, and squares represent the GliP T_3 mutant.

0.0130 ± 0.0006 min^{-1}. Furthermore, DKP formation is equally leisurely in wild type and in the T_3 and C_2 mutants, which indicates that the released DKP can be generated from the L-Phe-L-Ser-*S*-T_2 intermediate.

DISCUSSION

The 14 known members of the ETP fungal toxins all use a cyclic diketopiperazine as a scaffold that bears a 3,6-disulfide or 3,6-polysulfide bridge. The di/polysulfide functionality is the source of both higher eukaryotic and fungal toxicity. ETPs such as gliotoxin proceed to form mixed disulfides with many thiol-containing proteins and thus show nonspecific toxicity. Further, the dithio forms of ETPs are subject to reoxidation to the disulfide forms and undergo iterative redox cycles, generating reactive oxygen species as another facet of damage (*1*, *2*). Although all ETPs share this di- to polysulfide bridge as warhead, the DKP scaffold can vary between several combinations of Phe, Ser, Trp, Tyr, Gly, Ala, Thr, and Val, presumably reflecting NRPS selectivity of amino acid monomers (*1*).

Almost all previously described DKPs resulting from NRPSs have required proline to be the second amino acid residue. Expression of the first two modules of either gramicidin S or tyrocidine synthetases leads to formation of phenylalanylprolyl DKP in vitro (*33*, *42*). Considering the more natural system of indole alkaloids from *Aspergillus* and *Penicillium* spp., fumitremorgin B, in which the gene cluster is known to encode an NRPS, and the related molecules tryprostatins, cyclotryprostatins, spirotryprostatins, fumitremorgins, verruculogen, brevianamides, paraherquamides, and austamides all contain a DKP formed from L-Trp and L-Pro (*43*). Similarly, the ergot alkaloid ergotamine from *Claviceps purpurea*, for which the gene cluster encodes several NRPSs, contains a phenylalanylprolyl DKP precursor (*44*, *45*). Due to the presence of proline in all of these NRPS-derived products and the lack of thioesterase domains which normally catalyze terminal cyclization in NRPs, it is postulated that DKP formation may be spontaneous as a result of conformational constraints induced by the cyclic nature of proline and instability of the peptidyl thioester.

One notable exception to this requirement of proline for DKP formation in NRPs can be found in the biosynthesis of thaxtomins from *Streptomyces* spp. which consist of related congeners of cyclo-(L-4-nitrotryptophyl-L-phenylalanyl). How-

ever, in this system the amino acids are activated on separate NRPS proteins which have identical A-M-T-C organization (*46*). This may suggest some quaternary interaction between the NRPSs with both C domains acting in a concerted manner, thus bypassing a linear dipeptide intermediate. Additionally, DKPs have been known to arise independently of NRPSs. In mammals the DKP cyclo(L-His-L-Pro) is derived from the nonenzymatic cyclization of the thyrotropin-releasing hormone (TRH, pGlu-His-Pro) after cleavage by pyroglutamate amino peptidase (*47*). *Streptomyces noursei* produces a non-proline-containing DKP albonoursin, cyclo-(ΔPhe-ΔLeu). Sequencing of the gene cluster and functional analysis demonstrated that a small 26.8 kDa protein, AlbC, was capable of synthesizing the cylco(L-Phe-L-Leu) precursor as well as cyclo(L-Phe-L-Phe) when expressed in *Streptomyces lividans* and *E. coli* (*48*).

While the enzymatic machinery and mechanism for building the 3,6-disulfide bridge are key defining features of ETPs and as yet remain unstudied, the work reported here provides a starting point for understating the assembly of the DKP scaffold. First, we have achieved overproduction and purification of the *A. fumigatus* Af293 GliP three module NRPS in *E. coli*. This enormous 236 kDa protein can be coaxed into expression in soluble form and purified in usable quantities for initial enzymatic characterization. Second, we have been able to use the posttranslational priming enzyme Sfp, from *B. subtilis*, to convert the apo GliP to the holo GliP form, enabling study of peptide bond formation. To our knowledge GliP represents the first multimodular fungal NRPS to be successfully heterologously expressed in *E. coli* with production of soluble functional protein. Previously, multimodular NRPSs were purified directly from their fungal source, as was the case for enniatin synthetase purified from *Fusarium scirpi* (*49*) and ampullosporin synthetases purified from *Sepedonium ampullosporum* (*50*). However, these enzymes were only demonstrated to be functional for amino acid adenylation. Recently, a T-C didomain, Fum14p, from *Fusarium verticillioides* (*51*) was successfully heterologously expressed in *E. coli*; however, it was used to form ester bonds between two soluble substrates, not the typical enzyme-bound peptides found in NRPS assembly lines. Third, we have established that the A_1 domain activates L-Phe and the A_2 domain activates L-Ser, providing baseline information for fungal A domain selection rules. Fourth, we have established that the holo T_1 and T_2 domains become covalently loaded with L-Phe and L-Ser, respectively, and that C_1 condenses the L-Phe moiety from T_1 onto L-Ser-*S*-T_2 to yield the dipeptidyl L-Phe-L-Ser-*S*-T_2 enzyme intermediate.

At this point the role of the third, incomplete module C_2-T_3 is unclear. It is possible that dipeptidyl transfer to T_3 is part of normal catalysis. Mutational analysis of C_2 and T_3 suggests that they are involved in the same process because knocking out either domain yields identical HPLC profiles for intermediates that had been tethered to GliP, a profile that is distinct from wild-type GliP. Two new intermediates arise from these mutants. The first intermediate was positively identified as the phenylalanylseryl DKP using both coelution with authentic standard and mass spectrometry. Although the DKP cannot possibly be a tethered intermediate on GliP, this finding suggests that the mutant GliP may be stalled and present the L-Phe-L-Ser thioester in a conformation that results in intramolecular capture of the activated Ser carbonyl by the amino group of the L-Phe-L-Ser-*S*-T_2 under the particular assay conditions. The second new intermediate could not be identified to date. Several possible compounds were synthesized, but none coeluted nor did mass spectrometry yield any information as to the identity of the intermediate.

Our efforts to detect the dipeptidyl chain accumulating on T_3 have not yet succeeded, in part because of spontaneous DKP formation and release from GliP at a rate of approximately one per hour.

The absence of a TE domain in GliP is unusual but in fact may ensure that the only release route is the intramolecular cyclization to the cyclo-L-Phe-L-Ser DKP. DKP formation is observed in other NRPS assembly lines, but the conformer determinants that control intramolecular capture of the thioester by the amine in the dipeptidyl chain are not fully understood. Presumably, the other ETP biosynthetic NRPSs that make DKP scaffolds will have equivalent modular architecture, a presumption which does hold true for SirP, the NRPS involved in biosynthesis of sirodesmin (*21*). The NRPS encoding the cyclo-(L-Trp-L-Pro) known as brevianamide F in the biogenesis of the *A. fumigatus* tremorgenic mycotoxin fumitremorgin (*52*) has recently been observed to be a bimodular enzyme with an extra C domain (A_1-T_1-C_1-A_2-T_2-C_2). The role of the last C domain in generation or release of the DKP scaffold is not yet known since no studies on the purified DKP synthetase have yet been reported.

Whether intramolecular cyclization and turnover to free DKP are fast in vivo or in the presence of other proteins for fashioning the ETP core is not yet clear. It is also possible, albeit without any experimental evidence, that the sulfur incorporation occurs before cyclization to DKP, for example, while the L-Phe-L-Ser dipeptide is tethered on T_3. Future work with other enzymes in the gliotoxin cluster will involve assays both with the free DKP and with intermediates tethered on wild type and mutant forms of GliP.

ACKNOWLEDGMENT

We thank Dr. Robert A. Cramer, Jr., for providing us with *A. fumigatus* Af293 cDNA. We also thank Dr. Darren Hansen for a careful reading of the manuscript.

REFERENCES

1. Gardiner, D. M., Waring, P., and Howlett, B. J. (2005) The epipolythiodioxopiperazine (ETP) class of fungal toxins: distribution, mode of action, functions and biosynthesis, *Microbiology 151*, 1021−1032.
2. Waring, P., and Beaver, J. (1996) Gliotoxin and related epipolythiodioxopiperazines, *Gen. Pharmacol. 27*, 1311−1316.
3. De Clercq, E., Billiau, A., Ottenheijm, H. C., and Herscheid, J. D. (1978) Antireverse transcriptase activity of gliotoxin analogs, *Biochem. Pharmacol. 27*, 635−639.
4. Rightsel, W. A., Schneider, H. G., Sloan, B. J., Graf, P. R., Miller, F. A., Bartz, O. R., Ehrlich, J., and Dixon, G. J. (1964) Antiviral activity of gliotoxin and gliotoxin acetate, *Nature 204*, 1333−1334.
5. Rodriguez, P. L., and Carrasco, L. (1992) Gliotoxin: inhibitor of poliovirus RNA synthesis that blocks the viral RNA polymerase 3Dpol, *J. Virol. 66*, 1971−1976.
6. Mullbacher, A., and Eichner, R. D. (1984) Immunosuppression in vitro by a metabolite of a human pathogenic fungus, *Proc. Natl. Acad. Sci. U.S.A. 81*, 3835−3837.
7. Mullbacher, A., Waring, P., and Eichner, R. D. (1985) Identification of an agent in cultures of *Aspergillus fumigatus* displaying

anti-phagocytic and immunomodulating activity in vitro, *J. Gen. Microbiol. 131*, 1251−1258.
8. Mullbacher, A., Waring, P., Tiwari-Palni, U., and Eichner, R. D. (1986) Structural relationship of epipolythiodioxopiperazines and their immunomodulating activity, *Mol. Immunol. 23*, 231−235.
9. Beaver, J. P., and Waring, P. (1994) Lack of correlation between early intracellular calcium ion rises and the onset of apoptosis in thymocytes, *Immunol. Cell Biol. 72*, 489−499.
10. Suhadolnik, R. J., and Chenowith, R. G. (1958) Biosynthesis of gliotoxin. I. Incorporation of phenylalanine-1- and -2-C^{14}, *J. Am. Chem. Soc. 80*, 4391−4392.
11. Winstead, J. A., and Suhadolnik, R. J. (1960) Biosynthesis of gliotoxin. II. Further studies on the incorporation of carbon-14 and tritium-labeled precursors, *J. Am. Chem. Soc. 82*, 1644−1647.
12. Bu'Lock, J. D., and Leigh, C. (1975) Biosynthesis of gliotoxin, *J. Chem. Soc., Chem. Commun.* 628−629.
13. Kirby, G. W., Graham, P. L., and Robins, D. J. (1978) *cyclo*-(L-Phenylalanyl-L-seryl) as an intermediate in the biosynthesis of gliotoxin, *J. Chem. Soc., Perkin Trans. I 11*, 1336−1338.
14. Behling, R. A., and Fischer, A. G. (1980) Formation of phenylalanylserine and cyclo-phenylalanylseryl by protoplasts of *Gliocladium virens*, *Int. J. Biochem. 11*, 457−458.
15. Macdonald, J. C., and Slater, G. P. (1975) Biosynthesis of gliotoxin and mycelianamide, *Can. J. Biochem. 53*, 475−478.
16. Holden, M. T., Ram Chhabra, S., de Nys, R., Stead, P., Bainton, N. J., Hill, P. J., Manefield, M., Kumar, N., Labatte, M., England, D., Rice, S., Givskov, M., Salmond, G. P., Stewart, G. S., Bycroft, B. W., Kjelleberg, S., and Williams, P. (1999) Quorum-sensing cross talk: isolation and chemical characterization of cyclic dipeptides from *Pseudomonas aeruginosa* and other gram-negative bacteria, *Mol. Microbiol. 33*, 1254−1266.
17. Park, D. K., Lee, K. E., Baek, C. H., Kim, I. H., Kwon, J. H., Lee, W. K., Lee, K. H., Kim, B. S., Choi, S. H., and Kim, K. S. (2006) Cyclo(Phe-Pro) modulates the expression of ompU in *Vibrio* spp., *J. Bacteriol. 188*, 2214−2221.
18. Strom, K., Sjogren, J., Broberg, A., and Schnurer, J. (2002) *Lactobacillus plantarum* MiLAB 393 produces the antifungal cyclic dipeptides cyclo(L-Phe-L-Pro) and cyclo(L-Phe-trans-4-OH-L-Pro) and 3-phenyllactic acid, *Appl. Environ. Microbiol. 68*, 4322−4327.
19. Fdhila, F., Vazquez, V., Sanchez, J. L., and Riguera, R. (2003) dd-diketopiperazines: antibiotics active against *Vibrio anguillarum* isolated from marine bacteria associated with cultures of *Pecten maximus*, *J. Nat. Prod. 66*, 1299−1301.
20. Gardiner, D. M., and Howlett, B. J. (2005) Bioinformatic and expression analysis of the putative gliotoxin biosynthetic gene cluster of *Aspergillus fumigatus*, *FEMS Microbiol. Lett. 248*, 241−248.
21. Gardiner, D. M., Cozijnsen, A. J., Wilson, L. M., Pedras, M. S., and Howlett, B. J. (2004) The sirodesmin biosynthetic gene cluster of the plant pathogenic fungus *Leptosphaeria maculans*, *Mol. Microbiol. 53*, 1307−1318.
22. Cramer, R. A., Jr., Gamcsik, M. P., Brooking, R. M., Najvar, L. K., Kirkpatrick, W. R., Patterson, T. F., Balibar, C. J., Graybill, J. R., Perfect, J. R., Abraham, S. N., and Steinbach, W. J. (2006) Disruption of a nonribosomal peptide synthetase in *Aspergillus fumigatus* eliminates gliotoxin production, *Eukaryot. Cell 5*, 972−980.
23. Cane, D. E., and Walsh, C. T. (1999) The parallel and convergent universes of polyketide synthases and nonribosomal peptide synthetases, *Chem. Biol. 6*, R319−R325.
24. Cane, D. E., Walsh, C. T., and Khosla, C. (1998) Harnessing the biosynthetic code: combinations, permutations, and mutations, *Science 282*, 63−68.
25. Marahiel, M. A., Stachelhaus, T., and Mootz, H. D. (1997) Modular peptide synthetases involved in nonribosomal peptide synthesis, *Chem. Rev. 97*, 2651−2674.
26. Schwarzer, D., and Marahiel, M. A. (2001) Multimodular biocatalysts for natural product assembly, *Naturwissenschaften 88*, 93−101.
27. Stein, T., Vater, J., Kruft, V., Otto, A., Wittmann-Liebold, B., Franke, P., Panico, M., McDowell, R., and Morris, H. R. (1996) The multiple carrier model of nonribosomal peptide biosynthesis at modular multienzymatic templates, *J. Biol. Chem. 271*, 15428−15435.
28. Weber, T., and Marahiel, M. A. (2001) Exploring the domain structure of modular nonribosomal peptide synthetases, *Structure 9*, R3−R9.
29. Conti, E., Stachelhaus, T., Marahiel, M. A., and Brick, P. (1997) Structural basis for the activation of phenylalanine in the nonribosomal biosynthesis of gramicidin S, *EMBO J. 16*, 4174−4183.
30. Stachelhaus, T., Huser, A., and Marahiel, M. A. (1996) Biochemical characterization of peptidyl carrier protein (PCP), the thiolation domain of multifunctional peptide synthetases, *Chem. Biol. 3*, 913−921.
31. Weber, T., Baumgartner, R., Renner, C., Marahiel, M. A., and Holak, T. A. (2000) Solution structure of PCP, a prototype for the peptidyl carrier domains of modular peptide synthetases, *Structure 8*, 407−418.
32. Belshaw, P. J., Walsh, C. T., and Stachelhaus, T. (1999) Aminoacyl-CoAs as probes of condensation domain selectivity in nonribosomal peptide synthesis, *Science 284*, 486−489.
33. Stachelhaus, T., Mootz, H. D., Bergendahl, V., and Marahiel, M. A. (1998) Peptide bond formation in nonribosomal peptide biosynthesis. Catalytic role of the condensation domain, *J. Biol. Chem. 273*, 22773−22781.
34. Sambrook, J., Fritsch, E. F., and Maniatis, T. (1989) *Molecular Cloning: A Laboratory Manual*, 2nd ed., Cold Spring Harbor Press, Painview, NY.
35. Quadri, L. E., Weinreb, P. H., Lei, M., Nakano, M. M., Zuber, P., and Walsh, C. T. (1998) Characterization of Sfp, a *Bacillus subtilis* phosphopantetheinyl transferase for peptidyl carrier protein domains in peptide synthetases, *Biochemistry 37*, 1585−1595.
36. Ho, S. N., Hunt, H. D., Horton, R. M., Pullen, J. K., and Pease, L. R. (1989) Site-directed mutagenesis by overlap extension using the polymerase chain reaction, *Gene 77*, 51−59.
37. Stachelhaus, T., Mootz, H. D., and Marahiel, M. A. (1999) The specificity-conferring code of adenylation domains in nonribosomal peptide synthetases, *Chem. Biol. 6*, 493−505.
38. Di Vincenzo, L., Grgurina, I., and Pascarella, S. (2005) In silico analysis of the adenylation domains of the freestanding enzymes belonging to the eucaryotic nonribosomal peptide synthetase-like family, *FEBS J. 272*, 929−941.
39. Keating, T. A., and Walsh, C. T. (1999) Initiation, elongation, and termination strategies in polyketide and polypeptide antibiotic biosynthesis, *Curr. Opin. Chem. Biol. 3*, 598−606.
40. Bergendahl, V., Linne, U., and Marahiel, M. A. (2002) Mutational analysis of the C-domain in nonribosomal peptide synthesis, *Eur. J. Biochem. 269*, 620−629.
41. Kohli, R. M., and Walsh, C. T. (2003) Enzymology of acyl chain macrocyclization in natural product biosynthesis, *Chem. Commun. (Cambridge)*, 297−307.
42. Stachelhaus, T., and Walsh, C. T. (2000) Mutational analysis of the epimerization domain in the initiation module PheATE of gramicidin S synthetase, *Biochemistry 39*, 5775−5787.
43. Grundmann, A., and Li, S. M. (2005) Overproduction, purification and characterization of FtmPT1, a brevianamide F prenyltransferase from *Aspergillus fumigatus*, *Microbiology 151*, 2199−2207.
44. Haarmann, T., Ortel, I., Tudzynski, P., and Keller, U. (2006) Identification of the cytochrome P450 monooxygenase that bridges the clavine and ergoline alkaloid pathways, *ChemBioChem 7*, 645−652.
45. Haarmann, T., Machado, C., Lubbe, Y., Correia, T., Schardl, C. L., Panaccione, D. G., and Tudzynski, P. (2005) The ergot alkaloid gene cluster in *Claviceps purpurea*: extension of the cluster sequence and intra species evolution, *Phytochemistry 66*, 1312−1320.
46. Healy, F. G., Wach, M., Krasnoff, S. B., Gibson, D. M., and Loria, R. (2000) The txtAB genes of the plant pathogen *Streptomyces acidiscabies* encode a peptide synthetase required for phytotoxin thaxtomin A production and pathogenicity, *Mol. Microbiol. 38*, 794−804.
47. Moss, J., and Bundgaard, H. (1990) Kinetics and mechanism of the facile cyclization of histidyl-prolineamide to cyclo(His-Pro) in aqueous solution and the competitive influence of human plasma, *J. Pharm. Pharmacol. 42*, 7−12.
48. Lautru, S., Gondry, M., Genet, R., and Pernodet, J. L. (2002) The albonoursin gene cluster of S noursei biosynthesis of diketopiperazine metabolites independent of nonribosomal peptide synthetases, *Chem. Biol. 9*, 1355−1364.
49. Glinski, M., Urbanke, C., Hornbogen, T., and Zocher, R. (2002) Enniatin synthetase is a monomer with extended structure: evidence for an intramolecular reaction mechanism, *Arch. Microbiol. 178*, 267−273.

50. Reiber, K., Neuhof, T., Ozegowski, J. H., von Dohrend, H., and Schwecke, T. (2003) A nonribosomal peptide synthetase involved in the biosynthesis of ampullosporins in *Sepedonium ampullosporum*, *J. Pept. Sci. 9*, 701−713.

51. Zaleta-Rivera, K., Xu, C., Yu, F., Butchko, R. A., Proctor, R. H., Hidalgo-Lara, M. E., Raza, A., Dussault, P. H., and Du, L. (2006) A bidomain nonribosomal peptide synthetase encoded by FUM14 catalyzes the formation of tricarballylic esters in the biosynthesis of fumonisins, *Biochemistry 45*, 2561−2569.

52. Maiya, S., Grundmann, A., Li, S. M., and Turner, G. (2006) The fumitremorgin gene cluster of *Aspergillus fumigatus*: identification of a gene encoding brevianamide F synthetase, *ChemBioChem* (in press).

BI061845B